

## A review on photo-mediated ultrasound therapy

Rohit Singh  and Xinmai Yang

Department of Mechanical Engineering, Institute for Bioengineering Research, The University of Kansas, Lawrence, KS 66045, USA  
Corresponding author: Xinmai Yang. Email: xmyang@ku.edu

### Impact Statement

Photo-mediated ultrasound therapy (PUT) is a newly developed therapeutic technology. This technology has the potential to treat several diseases such as diabetic retinopathy, age-related macular degeneration, port-wine stains, and deep-vein thrombosis. Several experimental and numerical studies were conducted in the last decade to advance the PUT. This article briefly summarizes the therapeutic effects observed during the *in vivo* studies and the working mechanisms of PUT investigated through numerical and *in vitro* studies. The challenges in clinical translation of PUT and PUT-based technologies are also discussed. Therefore, this mini-review will foster future research on PUT.

### Abstract

Photo-mediated ultrasound therapy (PUT) is a novel therapeutic technique based on the combination of ultrasound and laser. The underlying mechanism of PUT is the enhanced cavitation effect inside blood vessels. The enhanced cavitation activity can result in bio-effects such as reduced perfusion in microvessels. The reduced perfusion effect in microvessels in the eye has the potential to control the progression of eye diseases such as diabetic retinopathy and age-related macular degeneration. Several *in vivo* studies have demonstrated the feasibility of PUT in removing microvasculature in the eye using rabbit eye model and vasculature in the skin using rabbit ear model. Numerical studies using a bubble dynamics model found that cavitation is enhanced during PUT due to the dramatic increase in size of air/vapor nuclei in blood. In addition, the study conducted to model cavitation dynamics inside a blood vessel during PUT found stresses induced on the vessel wall during PUT are higher than that at normal physiological levels, which may be responsible for bio-effects. The concentration of vasodilators such as nitric oxide and prostacyclin were also found to be affected during PUT in an *in vitro* study, which may limit blood perfusion in vessels. The main advantage of PUT over conventional techniques is non-invasive, precise, and selective removal of

microvessels with high efficiency at relatively low energy levels of ultrasound and laser, without affecting the nearby structures. However, the main limitation of vessel rupture/hemorrhage needs to be overcome through the development of real-time monitoring of treatment effects during PUT. In addition to the application in removing microvessels, PUT-based techniques were also explored in treating other diseases. Studies have found a combination of ultrasound and laser to be effective in removing blood clots inside veins, which has the potential to treat deep-vein thrombosis. The disruption of atherosclerotic plaque using combined ultrasound and laser was also tested, and the feasibility was demonstrated.

**Keywords:** Photo-mediated ultrasound therapy, ultrasound, laser, photoacoustic, cavitation, anti-vascular, thrombolysis, Keller–Miksis equation, finite element model, shear and circumferential stresses, vasodilators

**Experimental Biology and Medicine 2023; 248: 775–786. DOI: 10.1177/15353702231181191**

### Introduction

Ultrasonic cavitation is the formation, oscillation, and collapse of gas or vapor bubbles in a liquid upon the application of ultrasound wave. In the past few decades, numerous studies have been conducted to explore the therapeutic applications of ultrasound-induced cavitation. Cavitation-induced phenomena, including microstreaming,<sup>1</sup> microjets,<sup>2</sup> vessel-wall stresses,<sup>3</sup> and free-radical formation, can have various therapeutic applications, such as targeted drug delivery, gene transfer, blood–brain barrier (BBB) opening, and thrombolysis. In many applications, therapeutic ultrasound contrast agents are used during ultrasound treatment as they act as cavitation nuclei or as drug and gene carriers

to the treatment region. A drug can be directly delivered to a specific tissue by loading the drug onto a contrast agent and then releasing it using ultrasound energy. Ultrasonic cavitation will help to release the drug and will also increase cell membrane permeability to better facilitate drug delivery to the target.<sup>4</sup> Similarly, contrast agents in the presence of ultrasound can be used for gene therapy.<sup>5</sup> Drug and gene delivery are challenging for brain disorders, as the BBB blocks 100% of large-molecules and 98% of small-molecules administered neurotherapeutics.<sup>6</sup> Focused ultrasound along with contrast agents can transiently and non-invasively open the BBB to allow localized delivery of genes and drugs.<sup>7</sup> Another application of ultrasound cavitation is to dissolve blood clots in veins to treat deep-vein thrombosis (DVT), also known as

ultrasonic thrombolysis.<sup>8</sup> Blood clots can be dissolved by intravascular ultrasound, but it may cause damage to the vessel wall.<sup>8</sup> To overcome this, ultrasound can be combined with contrast agents to treat thrombosis at lower ultrasound amplitudes.<sup>9</sup> Moreover, thrombolytic drugs can also be carried by a contrast agent for better efficiency.<sup>10</sup> However, systemic injection of contrast agents in blood can have serious complications like toxicity at high concentration. Also, the treatment time window is limited by the circulation time of contrast agents.

We have developed a novel therapeutic technique that uses enhanced cavitation to induce bio-effects *in vivo*.<sup>11,12</sup> This technique does not require intravascular injection of contrast agent during ultrasound treatment; instead, a laser pulse is utilized synchronously with an ultrasound burst to initiate cavitation. This technique based on the combination of ultrasound and laser is known as PUT. PUT has its roots in photoacoustic (PA) or optoacoustic imaging.<sup>13</sup> In PA imaging (PAI), a nano-second pulsed laser illumination on tissue produces a sound wave or PA wave, which is detected by an ultrasound transducer. On the irradiation of a laser pulse, the chromophores in human tissue such as hemoglobin, melanin, water, and lipids absorb laser energy and convert it to heat, resulting in a temperature rise. This temperature increase produces thermoelastic expansion, which generates short acoustic pulses, also known as PA waves. As PA waves travel to the surface and are detected by an ultrasound transducer, an image can be reconstructed based on the arrival time and amplitude of the PA wave. The same principle of laser-induced PA wave is used in PUT, but the ultrasound transducer is used to send out acoustic burst in PUT rather than detecting the generated PA wave as in PAI.

PUT produces cavitation through photospallation based on PA cavitation.<sup>14,15</sup> The laser energy absorbed by the blood produces strong PA pressure. In the case of blood vessels, the laser-induced PA wave converges at the center, giving rise to significantly high rarefaction pressure near the center region of the vessel.<sup>16</sup> If an ultrasound burst is applied simultaneously, such that the laser-induced high rarefactional pressure is superimposed on the peak rarefaction phase of the ultrasound cycle, cavitation can be produced inside the blood vessel.<sup>17,18</sup> The nano-second laser pulse is used to initiate cavitation and the ultrasound wave drives the formed bubble. In PUT, enhanced cavitation is achieved at relatively low ultrasound amplitude with the irradiation of a nano-second laser pulse on the negative phase of the ultrasound cycle, without the injection of any contrast agent. The enhanced cavitation during PUT can be utilized to selectively shut-down microvessels without affecting surrounding tissues and structures.

The main potential application of PUT is to control the progression of neovascularization in the retinal<sup>19</sup> and choroidal<sup>20</sup> layers in the eye, which is useful in treating neovascularization-caused eye diseases such as diabetic retinopathy (DR) and age-related macular degeneration

(AMD). The other potential application of PUT is to reduce blood perfusion in microvessels of the skin,<sup>21</sup> which is useful in treating skin conditions such as port-wine stains (PWS). Apart from the anti-vascular effect of PUT, enhanced cavitation during PUT can be used to remove blood clots in veins<sup>22</sup> and plaque in arteries,<sup>23</sup> which can treat DVT and atherosclerosis. This review summarized studies conducted in the last decade during the advancement of the PUT technique and also discussed the clinical translation potential and challenges of PUT.

## Numerical studies

In the early studies of PUT, bio-effects such as reduction in vessel perfusion and hemorrhage were observed after the treatment.<sup>20,24</sup> The enhanced cavitation during PUT was believed to be the reason behind the bio-effects. The cavitation inside a blood vessel during ultrasound irradiation has been explored in various numerical studies. These studies calculated changes in bubble oscillation with variations in ultrasound parameters, initial bubble size, and blood vessel size.<sup>25,26</sup> Several studies have found stresses induced on vessel wall due to cavitation to be responsible for bio-effects induced during ultrasonic cavitation.<sup>27</sup> However, the mechanism of action of PUT was slightly different than traditional ultrasound-induced cavitation as laser beam was also used along with ultrasound in PUT. A few numerical studies have been conducted to explore cavitation dynamics during PUT.<sup>3,17,28</sup>

## Keller–Miksis equation coupled with diffusion equation

An early numerical study on PUT was conducted to study the changes in bubble size during combined irradiation of ultrasound and laser.<sup>17</sup> The bubble size was simulated by solving the Keller–Miksis equation (equations (1) and (2)).<sup>29</sup> The diffusion equation (equation (3)) was also coupled with the Keller–Miksis equation to include the effect of rectified diffusion in the bubble dynamics.<sup>30</sup> The bubble radius was calculated for irradiation with ultrasound-only and combined irradiation with ultrasound and laser (PUT). The changes in bubble size during PUT were calculated by including laser-induced PA wave along with ultrasound wave in the pressure driving  $\left( p \left( t + \frac{R}{c} \right) \right)$  term of the Keller–Miksis equation. The PA wave near the center of the blood vessel ( $0.001r_0$ ) due to laser irradiation was calculated using equation (4). The PA wave was superimposed on the peak negative phase of the ultrasound wave to result in a high-rarefaction pressure (Figure 1). This combined pressure was used as the driven pressure in the Keller–Miksis equation. Also, the results from equation (4) showed that the PA wave rarefactional pressure increased as blood vessel size increased and laser pulse-width decreased

$$\left( 1 - \frac{\dot{R}}{c} \right) R \ddot{R} + \frac{3}{2} \left( 1 - \frac{\dot{R}}{3c} \right) \dot{R}^2 = \frac{R}{\rho c} \frac{d}{dt} (P_b) + \frac{1}{\rho} \left( 1 + \frac{\dot{R}}{c} \right) \left( P_b - P_\infty - p \left( t + \frac{R}{c} \right) \right) \quad (1)$$

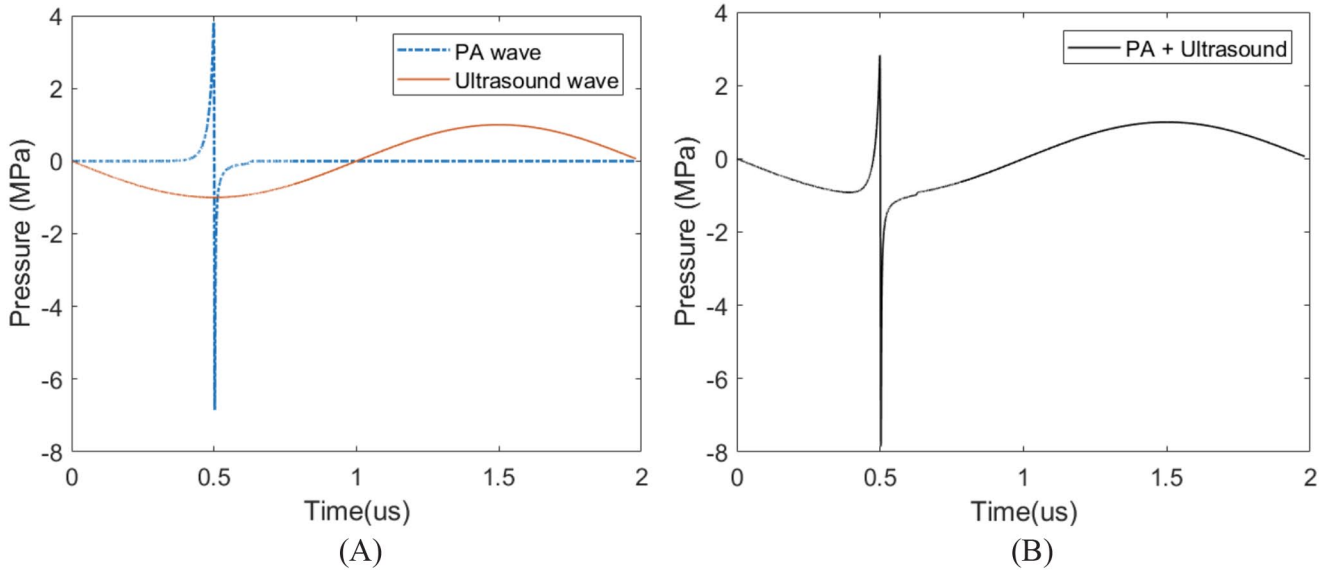


**Figure 1.** (A) Illustration of the applied laser-induced photoacoustic (PA) wave and ultrasound waveform separately. (B) Total driving pressure (photoacoustic (PA) + ultrasound). The ultrasound peak amplitude was 0.8 MPa, and laser fluence was 20 mJ/cm<sup>2</sup>. Adapted from Li *et al.*<sup>17</sup>

$$P_b = \left( P + \frac{2\sigma}{R_o} \right) \left( \frac{R_o}{R} \right)^{3k} \left( \frac{n}{n_o} \right) \left( \frac{R_{on}}{R_o} \right)^{3(n-1)} - \left( \frac{2\sigma}{R} \right) - \left( \frac{4\mu\dot{R}}{R} \right) \quad (2)$$

$$n = n_o - 4(\pi E)^{\frac{1}{2}} \int_0^{\tau} F(\tau') (\tau - \tau')^{\frac{1}{2}} d\tau' \quad (3)$$

$$p(r, t) = \frac{\int_{-\infty}^{+\infty} e^{\left(-\frac{2r'}{T}\right)^2} p_{\delta}(r, t - t') dt'}{\int_{-\infty}^{+\infty} e^{\left(-\frac{2r'}{T}\right)^2} dt'} \quad (4)$$

### Bubble growth during PUT

The size evolution of a 100 nm bubble was simulated.<sup>17</sup> The simulation results found that the bubble would dissolve in the presence of ultrasound field only (Figure 2(A)), whereas the bubble size increased dramatically when a laser pulse was combined with the first peak negative phase of the ultrasound burst (0–0.03 ms in Figure 2(B)). The bubble kept on growing in size in the subsequent ultrasound cycles through rectified diffusion until it reaches a large stable equilibrium radius (0–5.4 ms in Figure 2(B)). During the initial growth phase of the bubble, it increased in size by undergoing inertial cavitation. Then stable cavitation took place afterward, as shown in Figure 2(B) (5.97–6 ms). The ultrasound frequency also influenced the rate of growth/dissolution of the bubble, with higher frequency resulting in a faster dissolution rate, a slower growth rate, and a shorter time to reach stable cavitation. The observations were confirmed by experiments conducted on a 0.76 mm silicone tube filled with blood and irradiated with 0.243 MPa of 0.5 MHz ultrasound and 532 nm laser pulse with a fluence of 10 mJ/cm<sup>2</sup>.<sup>17</sup> In this study, the rectified diffusion thresholds for different bubble

sizes were also calculated using Fyrrillas and Szeri model.<sup>31</sup> The simulations found that the rectified diffusion threshold decreases with the addition of a laser pulse, and the decrease was greater with higher laser fluence. In other words, in the presence of a laser pulse, a relatively low amplitude ultrasound is required to drive a bubble to a larger size. Also, this effect was only significant for bubbles with a size less than 1000 nm.

### Shear and circumferential stresses

Earlier studies have found cavitation-induced stresses on vessel wall are responsible for bio-effects induced on blood vessels.<sup>27</sup> Inertial and non-inertial cavitation generate higher than physiological levels of shear and circumferential stresses inside blood vessels. The shear stress produces bio-effects such as activation of ion channels, reversible perforation of the membrane, and cell detachment and lysis,<sup>32</sup> whereas circumferential stress may result in vessel rupture and hemorrhage.<sup>33</sup> The magnitude of shear and circumferential stress directly impact the reduced perfusion in microvessels and hemorrhage observed in PUT.

### Finite element method model

Two numerical studies were conducted to calculate the changes in stresses induced on blood vessel wall during PUT.<sup>3,28</sup> In the first study, changes in circumferential and shear stresses were calculated when a laser pulse was combined with the first peak negative phase of an ultrasound burst.<sup>28</sup> The second study calculated the changes in stresses after the bubble achieved a large stable size in the later phase of an ultrasound burst.<sup>3</sup> In other words, the first study simulated the initial phase of PUT (0–0.03 ms in Figure 2(B)), when inertial cavitation took place and the second study simulated the later phase of PUT (5.97–6 ms in Figure 2(B)), when stable cavitation took place. A finite element method (FEM) model

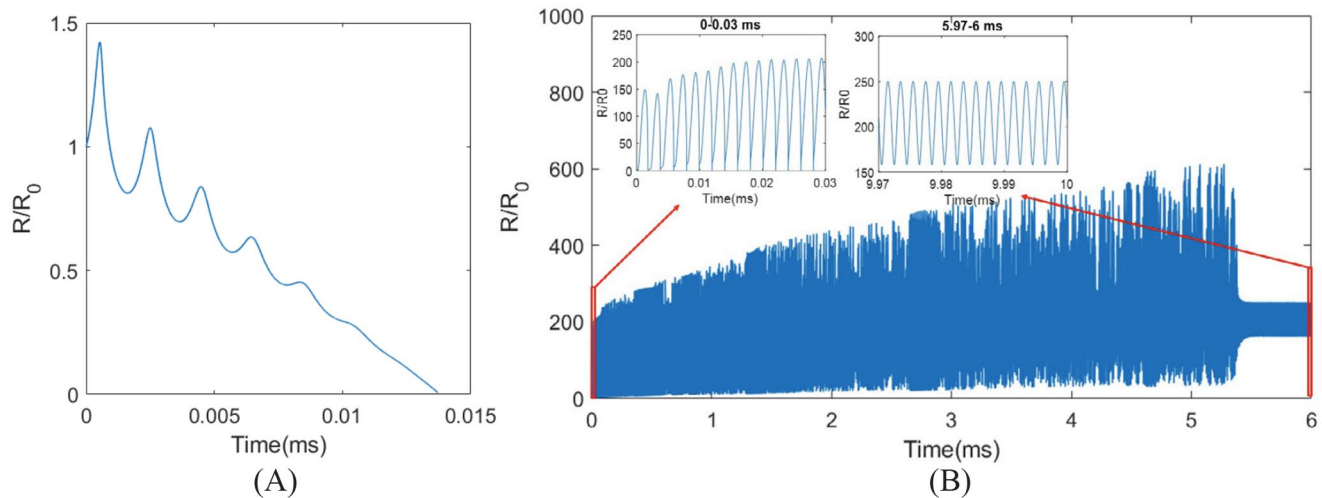


**Figure 2.** Simulated bubble size evolution under (A) ultrasound and (B) synchronized laser-induced photoacoustic wave and ultrasound.  $R_0$  was 100 nm, ultrasound frequency was 500 kHz, ultrasound peak amplitude was 0.8 MPa, and laser fluence was 20 mJ/cm<sup>2</sup>.  $R_0$ : initial bubble radius;  $R$ : bubble radius. Adapted from Li et al.<sup>17</sup>

was used to simulate cavitation during PUT in both studies. In the FEM model, an air bubble surrounded by blood was assumed inside a blood vessel, and the vessel was further surrounded by thick elastic tissues. To simplify the model, both air and blood were modeled as Newtonian fluids with air as compressible and blood as an incompressible fluid, and the vessel and tissue were modeled as isotropic linear elastic solids. The FEM model was developed and solved using the fluid–structure module in COMSOL-Multiphysics. Both ultrasound and laser-induced PA waves were used to drive the bubble to simulate the initial phase of PUT, while only ultrasound wave was used in the second study to simulate the stable cavitation phase of PUT as large size bubble oscillations are less affected by laser-induced PA wave.

In the first study, a small air/vapor bubble of size 50–100 nm was assumed to be present in the center of a blood vessel of size 50–150  $\mu\text{m}$ .<sup>28</sup> The bubble was assumed to be in the center of a blood vessel. Due to the symmetricity of the model around the vessel axis, it was solved with a 2D axisymmetric FEM model in COMSOL to save computation time. In the second study, to simulate the stable oscillation of a microbubble, a 2  $\mu\text{m}$  bubble was assumed to be present at different distances from the vessel center inside a 10  $\mu\text{m}$  vessel.<sup>3</sup> The off-center bubble was assumed because the bubble moves toward the vessel wall during the stable cavitation phase of PUT. Due to the off-center nature of the bubble, the FEM model was solved with a 3D FEM model in COMSOL. A small vessel size of only 10  $\mu\text{m}$  instead of large size was assumed in order to limit the computational time of the 3D model. Also a comparable bubble size of 2  $\mu\text{m}$  was used based on the vessel size of 10  $\mu\text{m}$ .

### Calculated stresses during PUT

Based on the 2D FEM model, the first study found that the addition of laser pulse on ultrasound burst produces much higher maximum circumferential and shear stresses on vessel wall as compared with ultrasound only.<sup>28</sup> For a 50 nm bubble inside a 50  $\mu\text{m}$  vessel, the irradiation with ultrasound

amplitude of 1.4–1.55 kPa at 1 MHz frequency produced shear and circumferential stresses less than 1 Pa and 2 kPa, respectively, on the vessel wall. In contrast, with the addition of a laser pulse of 20 mJ/cm<sup>2</sup> to the same ultrasound burst, the shear and circumferential stresses increased to 10–100 Pa and 100–400 kPa, respectively (Figure 3(A)), on the vessel wall. However, this increase in stresses during PUT was only significant for bubbles smaller than 100 nm in size (Figure 3(B)). Also, the produced stresses were found to decrease when ultrasound frequency and vessel size increased (Figure 3(A)). Based on the 3D FEM model, the second study found that the maximum circumferential and shear stresses increased as a bubble moved away from the center and toward the vessel wall.<sup>3</sup> The movement of a 2- $\mu\text{m}$  bubble from the center to the vicinity of a 10  $\mu\text{m}$  vessel resulted in more than 16 times (1.8–31.1 kPa) increase in shear stress (Figure 4(B)) and only 4 times (211 to 906 kPa) increase in circumferential stress (Figure 4(A)), in the presence of 130 kPa ultrasound wave of 1 MHz. Additionally, the stresses on vessel wall decreased as the bubble oscillation amplitude decreased. In summary, the studies using FEM models showed that the higher stresses induced on the vessel wall during PUT could be responsible for bio-effects observed in the *in vivo* studies. A larger increase in shear stress during bubble movement toward vessel wall in the later phase of PUT may have contributed to induce the desired bio-effects, while still limiting the chances of vessel rupture due to a smaller increase in circumferential stress. However, if the circumferential stress increases beyond the vessel rupture threshold, the vessel may rupture, resulting in hemorrhage.

In summary, the numerical studies showed that small air/vapor cavitation nuclei, which will otherwise dissolve in the presence of ultrasound,<sup>17</sup> in a blood vessel could grow dramatically in size due to combined irradiation of laser and ultrasound. During this growth of the bubble, it exerts higher circumferential and shear stresses on the blood vessel wall.<sup>28</sup> During PUT, the bubble will keep growing in size in the subsequent ultrasound cycles by rectified diffusion and

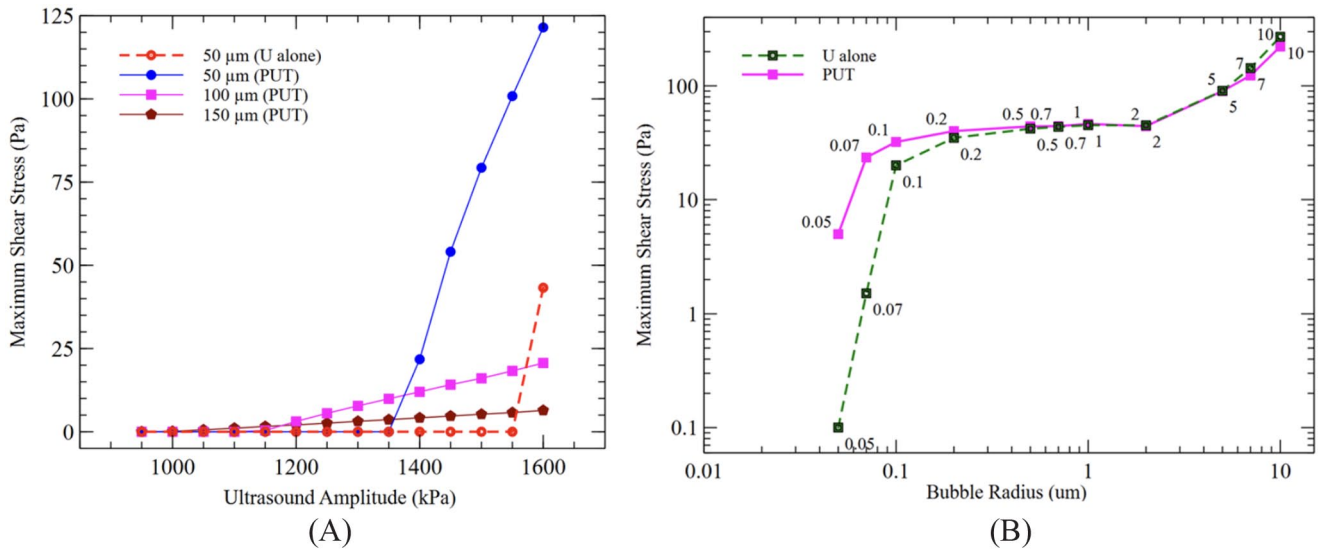


**Figure 3.** (A) Maximum shear stress as functions of the ultrasound amplitude for ultrasound alone and PUT on different size vessels (ultrasound frequency = 1 MHz, laser fluence = 20 mJ/cm<sup>2</sup>, and bubble radius = 50 nm; the negative peak of the PA wave was superposed on the ultrasound wave at a phase angle of 261° (at 725 ns), U: ultrasound). (B) Maximum shear stress on the wall of a 100 μm radius vessel as functions of the bubble radius for ultrasound and PUT (ultrasound amplitude = 1200 kPa, ultrasound frequency = 1 MHz, laser fluence = 20 mJ/cm<sup>2</sup>, and U: ultrasound). Adapted from Singh *et al.*<sup>28</sup>

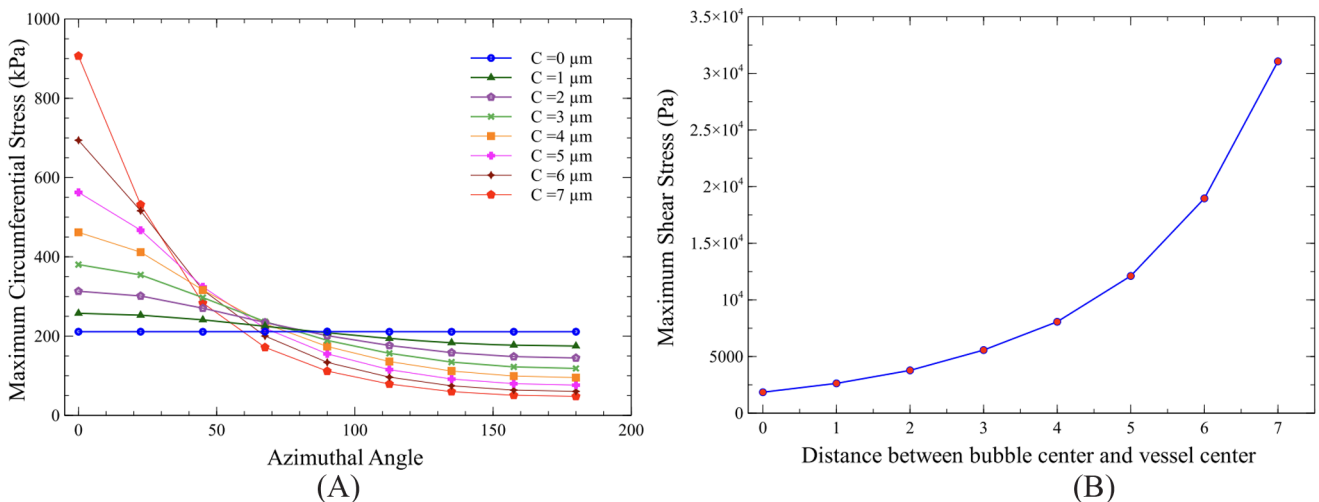


**Figure 4.** (A) Maximum circumferential stress as a function of the azimuthal angle for a 2 μm bubble placed at 0, 1, 2, 3, 4, 5, 6, and 7 μm away from the vessel center. (B) Maximum shear stress as a function of the distance between the bubble center and vessel center. (Peak ultrasound pressure = 130 kPa, ultrasound frequency = 1 MHz, vessel radius = 10 μm, and C = distance between the bubble center and vessel center.) Adapted from Singh *et al.*<sup>3</sup>

exhibit inertial cavitation behavior until it reaches a large stable size. The large stable cavitation during the rest of the ultrasound burst may slowly move toward the vessel wall, further increasing the stresses induced on vessel wall, with a greater increase in the shear stress and a smaller increase in circumferential stress.<sup>17</sup>

### In vitro study

#### Role of vasoactive agents in PUT

The changes in concentration of vasoactive agents inside blood vessels could play a role in the bio-effects observed during PUT. This was confirmed by a recent *in vitro* PUT study, in which an *in vitro* vessel model containing RF/6A

chorioretinal endothelial cells was treated with the combination of ultrasound and laser.<sup>34</sup> The concentrations of vasodilators such as nitric oxide and prostacyclin were measured after the treatments. It was found that the treatment with low energy levels of ultrasound-only and laser-only increases the release of nitric oxide and prostacyclin, whereas the combination of ultrasound and laser reduced the levels of increase in nitric oxide and prostacyclin. The reduction was related to the enhanced cavitation activity during PUT, which was confirmed with a passive cavitation detector during the experiment. The enhanced cavitation caused endothelial dysfunction, which causes reduction in increase of vasodilators, such as nitric oxide and prostacyclin, and ultimately reduces blood perfusion and shutdowns microvessels.

## PUT for non-cylindrical optical absorber

The PUT-related studies discussed above observed enhanced cavitation inside blood vessels due to its cylindrical shape, during combined irradiation of ultrasound and laser.<sup>17</sup> One study explored cavitation during PUT in slab-shaped optical absorbers using numerical simulation and *in vitro* experiments.<sup>35</sup> In the numerical model, the fluence at different positions was calculated using the Monte Carlo photon transport simulation.<sup>36</sup> The PA wave pressure resulted from laser absorption was calculated and used in the Keller–Miksis equation<sup>29</sup> to simulate bubble dynamics. An agar-based slab-shaped tissue phantom was used during *in vitro* experiments. The bottom half layer of the sample was dyed with black ink to increase optical absorption. Ultrasound bursts and laser pulses were focused to the top of the bottom layer of the sample and were moved between the light and dark sides of the sample. The study found enhancement in cavitation at the surface and deeper regions of the dark side of the bottom layer when a laser pulse was added to an ultrasound wave.<sup>35</sup> The study demonstrated that PUT could be effective in enhancing cavitation in non-cylindrical shaped soft tissues having sufficient optical absorption.

## *In vivo* studies with anti-vascular applications

Several studies on PUT were carried out with different *in vivo* models such as chicken embryo, rabbit ear, rabbit eye corneal vessels, rabbit eye choroidal vessels, and rabbit eye retinal vessels.<sup>19–21,24,37,38</sup> In these studies, animals were usually divided into PUT and control groups. In the PUT group, the treatment was conducted with combined ultrasound and laser, whereas in the control group, the treatment was conducted using ultrasound-only or laser-only. The same treatment parameters were used for both PUT and control groups. After the treatment, the PUT and control groups were monitored for up to four to six weeks (when possible) and the treated regions were evaluated for reduction in blood perfusion in microvessels.

## Experiment setup

Figure 5 shows a typical system schematic for a PUT system. The setup is a combination of a focused ultrasound (FUS) system and a pulsed nano-second laser system. The laser system used a standard Nd:laser (Continuum Powerlite DLS 8010, Santa Clara, CA) to produce 532 nm and 1064 nm wavelength lasers. For ultrasound, a FUS transducer with a central frequency of 0.5 MHz (H107, Sonic Concepts, Bothell, WA) or 1 MHz (H102, Sonic Concepts, Bothell, WA) was used. The 0.5 MHz FUS transducer has a focal distance of 63.2 mm, a focal depth of 21.42 mm, and a focal width of 3.02 mm.<sup>19–21,37</sup> The 1 MHz FUS transducer has a focal distance of 63.2 mm, a focal depth of 13.5 mm, and a focal width of 1.33 mm.<sup>24</sup> A delay generator (DG 535, Stanford Research Systems Inc., Sunnyvale, CA) was used to trigger both the ultrasound and laser systems. The trigger was supplied directly to the laser system and a function generator. The function generator (DS345, Stanford Research System, Sunnyvale, CA) produced the desired ultrasound burst,

which was first amplified by a power amplifier (2100L, E&I Technology Inc., Rochester, NY) and then supplied to the FUS transducer through an impedance matching network. The laser energy was adjusted by controlling the Q-switch delay time in the delay generator, and the ultrasound parameters such as amplitude, frequency, and duty cycle were controlled through the function generator.

## Synchronization and imaging

The laser and ultrasound systems were temporally synchronized such that the laser pulse overlaid the ultrasound burst during the first few cycles.<sup>18</sup> To ensure temporal synchronization, the traveling time of the ultrasound wave between the FUS transducer and treatment region was given as a delay to the ultrasound trigger in the delay pulse generator. The traveling time was measured by irradiating the treatment region with laser pulses and detecting the produced PA wave using the FUS transducer. The PA wave detected was first amplified in the pulser/receiver and then viewed on the oscilloscope by connecting it to connection 2 in Figure 5. The FUS transducer was connected to connection 1 during the treatment. Apart from temporal synchronization, the ultrasound burst and laser pulse were also spatially synchronized with the help of a 3D-printed conical cone. The cone was first attached to the FUS transducer and was filled with agar-gelatin-based couplant to provide acoustic coupling, as shown in Figure 5(B). A hole in the center of the cone was left for propagation of the laser beam. The cone was designed such that the FUS focal zone and laser beam coincided with the treatment region. For the treatment in rabbit eye, a real-time imaging system and a target laser beam were also incorporated into the experimental setup, as shown in Figure 5(B).<sup>19,20,37</sup> A charge-coupled device (CCD) was used to monitor the vasculature changes in rabbit eyes during the treatment. The illumination for imaging was provided by a mounted LED light (wavelength 565 nm, M565L3, Thorlabs). A He-Ne laser (wavelength 632.8 nm, HNL020LB, Thorlabs) was used to guide the treatment laser beam through the CCD image.

## Treatment parameters

The treatment parameters used in *in vivo* studies are listed in Table 1. In all the studies, a pulse repetition frequency of 10 Hz for both ultrasound burst and laser pulse was used.<sup>19–21,24,37</sup> The ultrasound frequency of 0.5<sup>19–21,37</sup> and 1 MHz<sup>24</sup> and an ultrasound amplitude in the range of 0.43–0.50 MPa<sup>19–21,24,37</sup> were used. The duty cycle was kept below 10% to keep thermal effects minimal during the treatment.<sup>19–21,24,37</sup> The laser wavelengths of 532,<sup>20,24</sup> 1064,<sup>19,21,37</sup> and 584 nm<sup>24</sup> were used due to strong absorption by blood at these wavelengths. The laser fluences for the chicken embryo study,<sup>24</sup> rabbit ear study,<sup>21,24</sup> and rabbit eye study<sup>19,20,37</sup> were 2–8, 20–56, and 27–85 mJ/cm<sup>2</sup>, respectively.

## Chicken yolk and rabbit ear model

The first *in vivo* study to test the combination of ultrasound and laser on microvessels was carried out on a chicken yolk sac membrane model and a rabbit ear model.<sup>24</sup> The blood

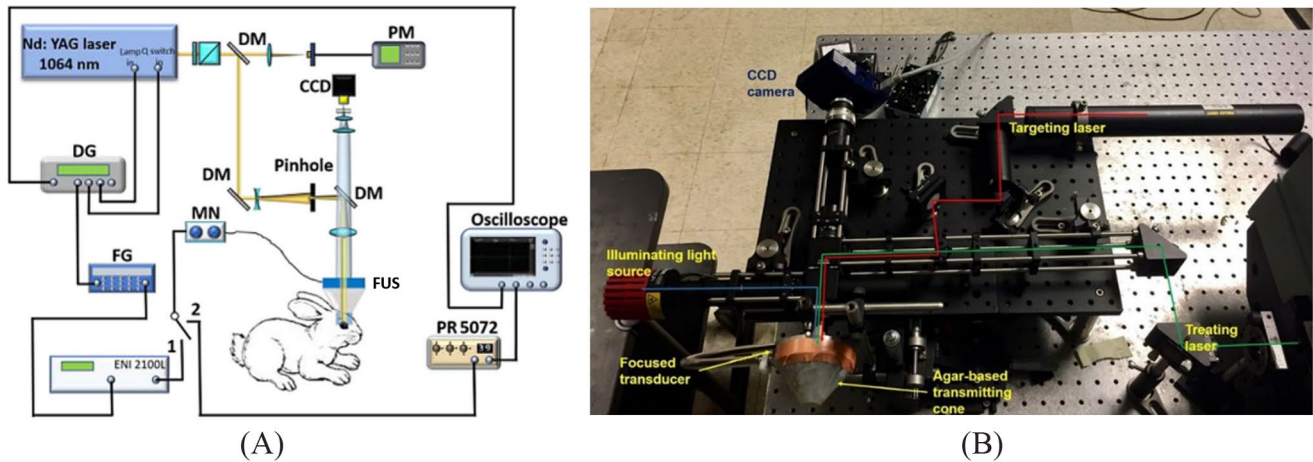


**Figure 5.** (A) Schematic of the experiment setup of the PUT system. Adapted from Qin *et al.*<sup>18</sup> (B) Photograph of the PUT treatment system. DM: dichroic mirrors; PM: power meter, DG: delay generator, FG: function generator, MN: matching network for FUS transducer, PR: pulser/receiver. Adapted from Zhang *et al.*<sup>20</sup>

**Table 1.** Ultrasound and laser treatment parameters for *in vivo* studies on photo-mediated ultrasound therapy (PUT).

	<i>In vivo</i> models					
	Rabbit eye model			Chicken embryo model <sup>24</sup>	Rabbit ear model <sup>24</sup> (2017 study)	Rabbit ear model <sup>21</sup> (2020 study)
	Choroidal <sup>20</sup>	Corneal <sup>37</sup>	Retinal <sup>19</sup>			
<b>Treatment parameters</b>						
Pulse repetition frequency (Hz)	10	10	10	10	10	10
<b>Ultrasound parameters</b>						
Frequency (MHz)	0.5	0.5	0.5	1	1	0.5
Amplitude (MPa)	0.5	0.43	0.48	0.45	0.45	0.45
Duty cycle (%)	10	10	5	10	10	0.2
<b>Laser parameters</b>						
Wavelength (nm)	532	1064	1064	532	584	1064
Pulse width (ns)	5	5	5	5	5	5
Beam diameter (mm)	1	3	3	8	8	3
Fluence (mJ/cm <sup>2</sup> )	55–75	27	85	2–8	20	56

vessel diameter before and after the PUT treatment were used for quantification of changes in blood perfusion. A laser wavelength of 532 nm and an ultrasound frequency of 1 MHz were used for the chicken yolk sac membrane model. Optical microscopic images were used for quantification of treatment results. The study found that PUT treatment using an ultrasound amplitude of 0.45 MPa along with laser fluences of 4, 6, and 8 mJ/cm<sup>2</sup> induced a vein reduction of 51%, 37%, and 90% in chicken yolk sac membrane. A laser wavelength of 584 nm and an ultrasound frequency of 1 MHz were used for the rabbit ear model. Laser speckle images were used to quantify the treatment outcomes. The rabbit auricular blood vessels treated with ultrasound amplitude of 0.45 MPa and laser fluence of 20 mJ/cm<sup>2</sup> were reduced by 68.5% at seven days after the treatment. The hematoxylin and eosin (H&E) stained histology was also carried out to confirm the treatment outcomes. In a more recent study on 38 auricular blood vessels of 4 rabbit ears, a 1064 nm wavelength laser of 56 mJ/cm<sup>2</sup> fluence and a 1 MHz frequency ultrasound of 0.45 MPa amplitude were used.<sup>21</sup> The laser speckle imaging was used to quantify the treatment outcomes. The vascular perfusion

was reduced by 50.79% immediately after the treatment. The perfusion was then rebounded slightly and the reduction in perfusion was around 30% after three days, and it maintained the same level (30%) until four weeks after the treatment.

### Rabbit eye model

The other PUT studies were conducted on rabbit eye models to test the PUT in reducing the blood perfusion of microvessels in the retina, choroid, and cornea.<sup>19,20,37</sup> The first PUT study on the eye was conducted using 22 rabbits to observe the PUT effects on choroidal vessels of the rabbit eye.<sup>20</sup> A FUS transducer of 0.5 MHz frequency at amplitude of 0.5 MPa and a 532 nm wavelength laser at a fluence of 55–75 mJ/cm<sup>2</sup> were used. Using fundus photographs, the number of choroidal vessels before and after the treatment were counted to quantify the treatment. The study found that the number of choroidal vessels was reduced by 72.89% ± 20.56% after the treatment, and the reduction was persisted for up to four weeks after the treatment. No treatment effect was observed

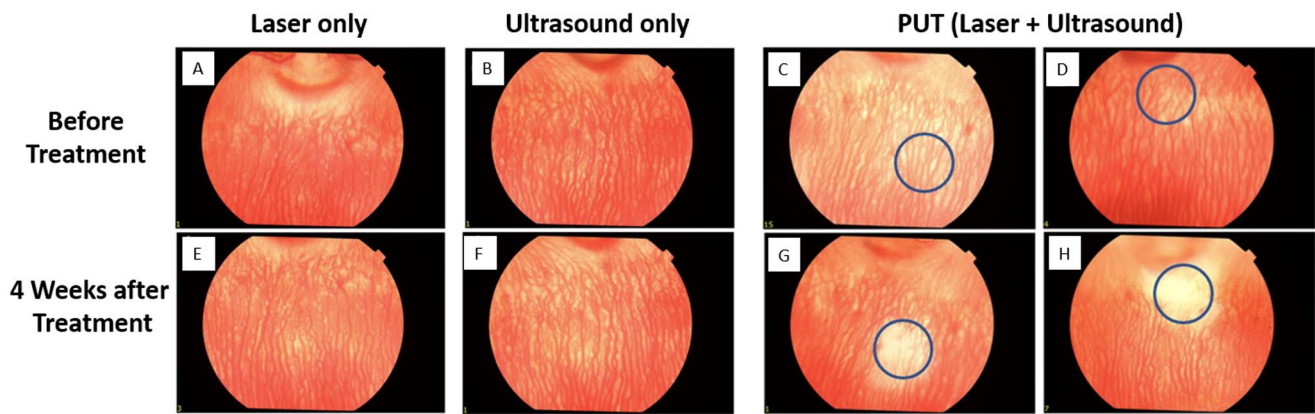


**Figure 6.** Fundus photograph of rabbit choroid before and four weeks after the treatment with laser only, ultrasound, and PUT: (A–D) Before treatment; (E–H) after treatment; (A, E) laser-only treatment; (B, F) ultrasound-only treatment; and (C, D, G, H) PUT treatment. Adapted from Zhang *et al.*<sup>20</sup>

after the treatment with ultrasound-only and laser-only. The results were confirmed by performing H&E stained histology on some of the treated eye sections. The choroid vessels before and four weeks after the treatment with laser-only, ultrasound-only, and PUT are shown in Figure 6. The second PUT study on rabbit eyes was conducted to test its efficiency in removing neovascularization in the cornea.<sup>37</sup> In this study, a corneal neovascularization (CNV) model in rabbit eyes was created and it was treated at a time period of seven weeks after CNV induction. A combination of 1064 nm laser at a fluence of 27 mJ/cm<sup>2</sup> and 0.5 MHz ultrasound at an amplitude of 0.43 MPa were used for all the treatments. To evaluate the treatment effects of PUT, the red-free photography and fluorescein angiography were used. To ensure the safety of PUT, the H&E stained histology and immunohistochemistry were carried out. After the treatment with PUT, only 1.8% ± 0.8% of the CNV remained at 30 days after the treatment, whereas 71.4% ± 7.2% of the CNV remained in the control group. In a more recent study, PUT was also tested for removing neovascularization in the retina.<sup>19</sup> A retinal neovascularization (RNV) model was created in eyes of albino and pigmented rabbits through injecting DL- $\alpha$ -amino adipic acid. The rabbits were treated with PUT eight weeks after the injection of DL- $\alpha$ -amino adipic acid using a 0.5 MHz ultrasound at amplitude of 0.48 MPa and a 1064 nm laser at fluence of 85 mJ/cm<sup>2</sup>. The treatment results were evaluated using fundus photography, red-free fundus photography, fluorescein angiography, and histopathology. At six weeks after the PUT treatment, only 9.9% ± 9.8% of the neovascularization remained in albino rabbits, and only 10.8% ± 9.8% of the neovascularization remained in the pigmented rabbits.

### Other PUT-based techniques

Apart from anti-vascular application of PUT, the enhanced cavitation observed in non-cylindrical shaped tissues has the potential to treat other medical conditions. Several studies have explored the use of combined ultrasound and laser to disrupt blood clots and atherosclerotic plaques.<sup>22,23,39,40</sup> These studies demonstrated the application of PUT-based therapy in treating DVT and atherosclerosis.

### Ultrasound-assisted endovascular laser thrombolysis

DVT is the formation of blood clots (thrombus) in the deep veins of the legs or pelvis. It can be life threatening if the clot breaks loose and travels to the lungs. Apart from traditional clinical therapies such as anticoagulant<sup>41</sup> and thrombolytic therapy,<sup>42</sup> ultrasound-based,<sup>43</sup> and laser-based techniques<sup>44</sup> have been evaluated to treat DVT. However, ultrasound-based and laser-based techniques were not successful in clinics due to their limitations. Ultrasound-based thrombolysis damages surrounding tissue and vessel wall;<sup>45</sup> and laser-based thrombolysis does not efficiently clear the thrombus occlusion inside the vein.<sup>46</sup> The combination of ultrasound and laser for thrombolysis was explored in several studies to overcome the current limitation of individual ultrasound-based and laser-based techniques.

The first study was conducted on an *in vitro* bovine blood clot model.<sup>39</sup> It was found that thrombolysis efficiency increased when a laser pulse was used concurrently with ultrasound waves. This was one of the preliminary studies during the early development stage of PUT. After better understanding of PUT mechanism through several studies, recently, studies were conducted on *in vitro* and *in vivo* models to demonstrate the thrombolysis using combined ultrasound and laser.<sup>22,40</sup> This PUT-based technology for thrombolysis was named as ultrasound-assisted endovascular laser thrombolysis (USELT). PUT and USELT are both based on the combination of ultrasound and laser. In PUT, both ultrasound and laser are delivered non-invasively to remove the microvessels, whereas in USELT, a laser pulse is delivered directly to the blood clot using a catheter and ultrasound is delivered non-invasively to achieve blood clot disruption/removal inside vein. The first study using USELT, where FUS at 0.5 MHz and pulsed nano-second laser light of 532 nm at 10 kHz pulse repetition frequency were used, was conducted on an *in vitro* blood flow clot model.<sup>40</sup> It was found that 1.26 MPa ultrasound amplitude was needed for thrombolysis with FUS only, whereas with the addition of 2 and 4 mJ/cm<sup>2</sup> of laser to FUS, only 1.05 and 0.59 MPa of FUS amplitude, respectively, was sufficient for effective thrombolysis. Also, the time required for

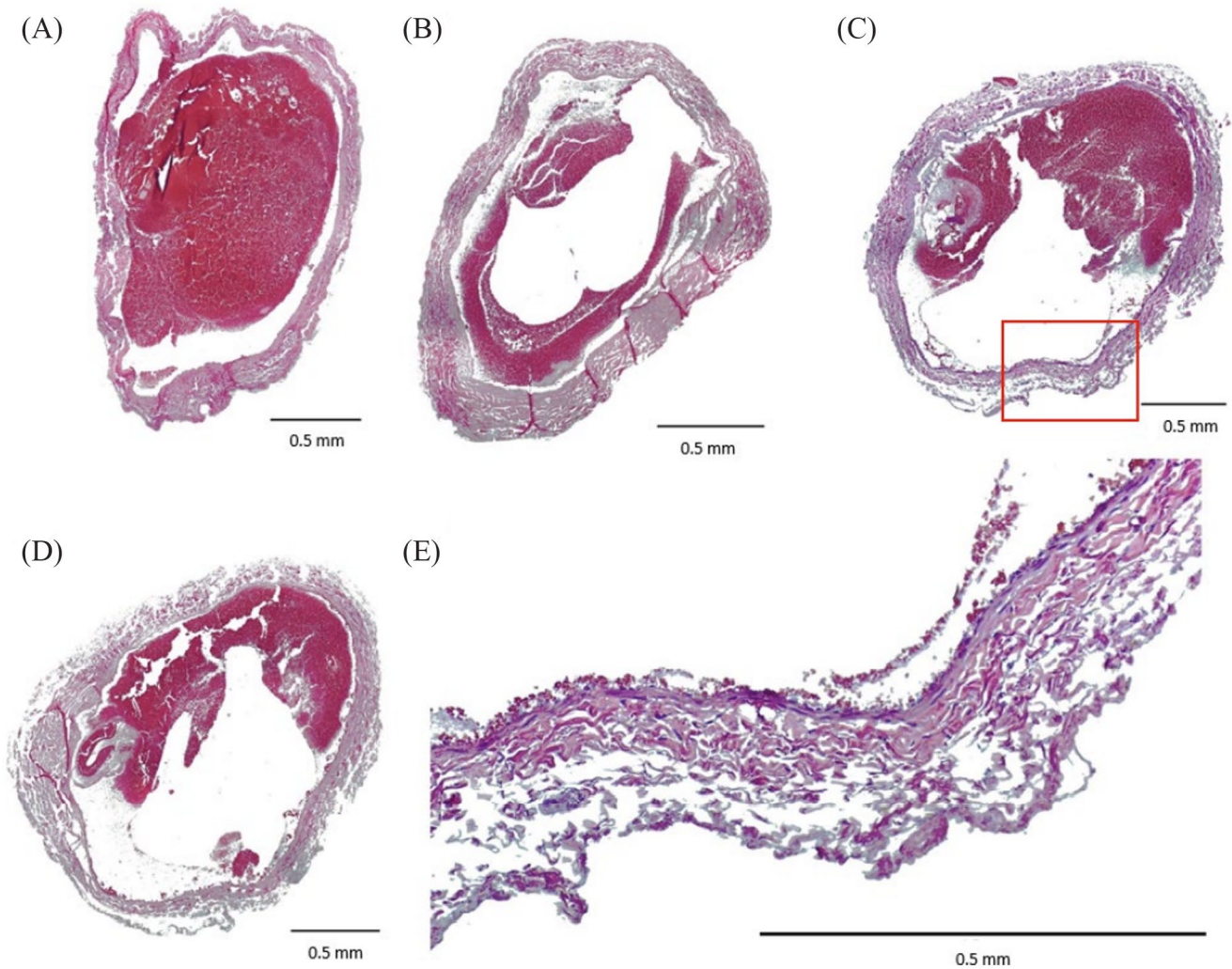


**Figure 7.** (A) Histology image (hematoxylin and eosin stain) of vein section treated with ultrasound only using P of 1.3 MPa. (B–D) Histology images (hematoxylin and eosin stain) of vein sections treated with USELT using ultrasound amplitude of 1 MPa and laser fluence of 12 mJ/cm<sup>2</sup>. (E) Magnified image of the highlighted area in the red box in (C). Ultrasound frequency was 500 kHz and laser wavelength was 532 nm. Adapted from Singh *et al.*<sup>22</sup> USELT: ultrasound-assisted endovascular laser thrombolysis.

effective thrombolysis was less when higher laser power and ultrasound amplitude were used. A following study on USELT was conducted on an *in vivo* rabbit blood clot model.<sup>22</sup> The blood clots were created in the jugular vein of rabbits and were treated with ultrasound-only, laser-only, and USELT. The ultrasound amplitude of 1.3 MPa and laser fluence of 8 mJ/cm<sup>2</sup> were used. Out of seven rabbits treated with USELT, the vein was completely recanalized (100%) in three rabbits; partially recanalized (70%) in two rabbits, and poorly recanalized (6%) in the other two rabbits. In contrast, in all the five rabbits treated with ultrasound-only and laser-only, no recanalization of veins took place. The histology results also confirmed the removal of blood clots in USELT treatment. Also, no damage to vessel wall was observed in the histology images of USELT treated veins as shown in Figure 7. Both the *in vitro* and *in vivo* studies on USELT demonstrated its potential in efficient removal of clot in DVT without causing any damage to the nearby tissues.

#### Ultrasound-assisted laser technique to remove atherosclerotic plaque

Atherosclerosis is a disease affecting the arteries, in which arteries harden and narrow due to the buildup of cholesterol, fat, calcium, and other substances. Apart from traditional atherosclerosis treatments such as angioplasty,<sup>47</sup> laser-based therapy known as excimer laser coronary angioplasty (ELCA) was also used in clinics to treat atherosclerosis.<sup>48</sup> However, clinical use of ELCA is limited due to its less efficiency in plaque removal and higher chances of developing complications.<sup>49</sup> The limitations of ELCA may be overcome by combining ultrasound with laser-based treatment. The combined ultrasound and laser treatment were tested to remove the atherosclerotic plaque in a recent study.<sup>23</sup> The experiments were performed on pig-belly fat and carotid artery plaque samples. The results found that addition of ultrasound reduces the needed laser power for treatment, which could improve efficiency and safety of treatment. In future *in vivo* studies for treating atherosclerosis, the laser

can be delivered directly to the plaque using a catheter, and ultrasound can be applied non-invasively from outside the body, similar to USELT. However, the laser fluence and ultrasound amplitude for atherosclerosis technique will be very different from USELT for blood clot removal, due to the difference in light absorption and mechanical properties between blood clots and plaques.

### Other techniques with combined ultrasound and laser

Other therapeutic techniques based on the combination of ultrasound and laser were also developed. Several studies focused on the development of a novel method to generate cavitation using combination of ultrasound and laser along with nanoparticles.<sup>50,51</sup> In the experiment, the light absorptive gold nanoparticles were seeded in the optically transparent phantom and were irradiated by the combination of ultrasound and laser.<sup>50</sup> Cavitation was detected at a combination of 0.10 mJ/cm<sup>2</sup> laser fluence and 0.92 MPa ultrasound pressure, whereas the cavitation threshold for ultrasound-only was 4.5 MPa. This result was also confirmed by a numerical study.<sup>51</sup> The same numerical study also calculated the optimal laser pulse length and particle size for generating cavitation at the lowest possible laser energy and acoustic pressure.<sup>51</sup> An *in vitro* study using gold nanospheres to disrupt blood clots compared results between ultrasound-only, laser-only, and combined ultrasound and laser.<sup>52</sup> They found an increase in cavitation lifetime when laser pulse was irradiated at the peak negative pressure of ultrasound. A recent study developed a high-speed PUT system and integrated it with optical coherence tomography angiography (OCTA) for real-time imaging.<sup>53</sup> They used a 50 kHz pulsed laser for faster treatment and tested the integrated system on rabbit ear model.

## Clinical translation potential of PUT

### Current clinical treatments and opportunities for PUT

The main potential clinical application of PUT is to treat DR and AMD. In these diseases, the blindness is caused by the formation of abnormal new microvessels in retinal and choroidal layer of the eye. Currently, the most widely used treatment in clinics is the injection (often monthly) of anti-vascular endothelial growth factor (VEGF) agents, which inhibits neovascularization.<sup>54</sup> Anti-VEGF therapy is inconvenient as it requires monthly hospital visit for injections.<sup>55</sup> For patients responding poorly to anti-VEGF therapy, alternate therapies based on laser such as photodynamic therapy (PDT) and laser photocoagulation therapy (LPT) are also used. In PDT, photosensitizers are injected and irradiated by laser light of specific wavelength, causing selective destruction of vessels by photocytotoxic reaction.<sup>56</sup> However, photosensitizers are sensitive to sunlight, and patients are required to avoid the sun exposure for several days after PDT.<sup>57</sup> LPT uses millisecond pulse duration laser with high pulse energy to remove microvasculature through tissue heating.<sup>58</sup> The heat can destroy adjacent surrounding cells and results in serious complications such as retinal atrophy,

subretinal neovascularization, and subretinal fibrosis.<sup>59,60</sup> The newly developed PUT is different from the current treatment therapies. PUT is completely non-invasive unlike the anti-VEGF therapy which requires injection of anti-VEGF and PDT which requires injection of photosensitizers. PUT removes microvessels through the mechanical action of cavitation without causing any damage to the surrounding tissue unlike LPT which damages nearby tissues due to its thermal based treatment mechanism. The thermal effects during PUT are controlled to be minimal by maintaining a duty cycle of less than 10% during the entire treatment duration. This absence of thermal damage was confirmed by H&E stained sections of rabbit eye and ear tissues.

The other potential clinical application of PUT is to treat vascular malformations such as PWS. In PWS, the pink to dark red lesions is found in the head and neck region of newborns due to abnormal dilation of capillaries and post-capillary venules. In clinics, pulsed dye laser (PDL) therapy is the most widely used treatment for PWS. PDL treats the PWS region through selectively heating and destroying the capillaries using 577–595 nm laser, also known as selective photothermolysis.<sup>61</sup> However, PDL is not effective in treating deep vessels due to limited penetration depth of laser.<sup>62</sup> For treating deeper lesions, 1064 nm light is effective due to its high penetration depth.<sup>63</sup> However, the use of high laser energy for treating deeper lesions at 1064 nm can cause scarring.<sup>64</sup> PUT can be used to treat deeper lesions of PWS using combination of 1064 nm laser and ultrasound.<sup>21</sup> The laser energy required at 1064 nm in PUT is several orders less than the traditional therapy, preventing side effects such as scarring. The use of low laser pulse energy, complete non-invasiveness, and cavitation-based bio-effects are the advantages of PUT over the traditional therapies.

### Challenges in clinical translation of PUT

All the *in vivo* studies reported significant reduction in blood vessel perfusion after PUT treatment, and the reduction persisted for up to four to six weeks after the treatment, while no significant treatment effect was observed in the control groups, including treatment with ultrasound-only and laser-only. These studies demonstrated the potential of PUT in treating neovascularization-based diseases. A major challenge in the clinical translation of PUT is to minimize hemorrhage during treatment. In all the *in vivo* studies, the reported ultrasound and laser parameters, mainly ultrasound amplitude and laser fluence, were optimized before the treatment. A lower value than the optimized value resulted in no changes in vasculature, whereas a higher value resulted in vessel rupture. The vessel rupture causes hemorrhage in the treatment zone. In the study on chicken embryo model, only 10% of vessels were ruptured at laser fluence of 4 mJ/cm<sup>2</sup> and ultrasound amplitude of 0.45 MPa. However, when laser fluence was increased to 6 and 8 mJ/cm<sup>2</sup> while keeping the ultrasound amplitude (0.45 MPa) same, the vessels rupture rate increased to 60% and 90%, respectively.<sup>24</sup> Also, when ultrasound amplitude was increased from 0.45 to 0.6 MPa in the rabbit auricular blood vessel study, immediate rupture of all the blood vessels was observed.<sup>24</sup> In the study on rabbit eye retinal model, microhemorrhage in the choroidal layer

was also observed at one week after the PUT treatment and disappeared at six weeks after the treatment.<sup>20</sup> A microhemorrhage was also observed in a study conducted on corneal vessels of the rabbit eye.<sup>37</sup>

Microhemorrhage may be minimized by including a real-time imaging system in the PUT setup to provide real-time feedback during PUT.<sup>38,53</sup> One study developed a PA sensing (PAS) system for PUT and tested it on chicken yolk sac membrane model.<sup>38</sup> The PAS system was integrated with the PUT system such that the same FUS transducer and laser beam were used for PUT treatment as well as for PAS. It was found that the PA signal decreased when vessel perfusion decreased, remained unchanged for no vessel perfusion/size change, and abruptly increased when vessel ruptured. However, this study was conducted on a single posterior vitelline vein of chicken yolk sac membrane. The design of integrated PAS-PUT system and evaluation of PAS signal will be more challenging for complex *in vivo* biological structures such as eye vasculature. Other imaging technology that may be used to provide real-time feedback during PUT is optical coherence tomography (OCT), which is, however, still under investigation.<sup>53</sup>

The ultrasound pressure used in PUT is smaller than the pressure produced by diagnostic ultrasound. Therefore, it is theoretically possible to use a diagnostic ultrasound system as the ultrasound source for PUT. However, the frequency range of diagnostic ultrasound is slightly different than that used in PUT. We used frequency of less than 1 MHz for all the *in vivo* studies, whereas the frequency of diagnostic ultrasound is above 2 MHz.<sup>65</sup> Also, we used a pressure amplitude of less than 0.5 MPa for all the PUT treatments and the pressure amplitude for diagnostic ultrasound of 2 MHz can go up to 2.68 MPa based on the Food and Drug Administration (FDA) safe limit of 1.9 (Mechanical Index < 1.9).<sup>66</sup> In spite of the same ultrasound pressure range, the use of diagnostic ultrasound for PUT needs to be investigated due to the differences in operating frequency, burst period, and pulse repetition frequency.

## Conclusions and future outlook

Through *in vivo*, *in vitro*, and numerical studies, the newly developed PUT technology, which is based on the combination of ultrasound and laser, has demonstrated significant potentials for the treatment of several neovascularization-related diseases such as DR and AMD, as well as DVT and PWS. Overall, the development of PUT technology is still in its infant stage, and substantial development is needed to further optimize the technology for specific applications and future clinical translations. Moreover, the development of real-time image-guided PUT will greatly facilitate this translation process.

### AUTHORS' CONTRIBUTIONS

All the authors have contributed equally in writing and editing this article.

### DECLARATION OF CONFLICTING INTERESTS

The author(s) declared no potential conflicts of interest with respect to the research, authorship, and/or publication of this article.

### FUNDING

The author(s) disclosed receipt of the following financial support for the research, authorship, and/or publication of this article: This work was supported in part through a National Institutes of Health (NIH) grant (No. R01EY029489).

### ORCID ID

Rohit Singh  <https://orcid.org/0000-0002-8415-6728>

### REFERENCES

- Collis J, Manasseh R, Liovic P, Tho P, Ooi A, Petkovic-Duran K, Zhu Y. Cavitation microstreaming and stress fields created by microbubbles. *Ultrasonics* 2010;**50**:273–9
- Kodama T, Tomita Y. Cavitation bubble behavior and bubble–shock wave interaction near a gelatin surface as a study of *in vivo* bubble dynamics. *Appl Phys B* 2000;**70**:139–49
- Singh R, Yang X. A 3D finite element model to study the cavitation induced stresses on blood-vessel wall during the ultrasound-only phase of photo-mediated ultrasound therapy. *AIP Adv* 2022;**12**:045020
- Geers B, Dewitte H, De Smedt SC, Lentacker I. Crucial factors and emerging concepts in ultrasound-triggered drug delivery. *J Control Release* 2012;**164**:248–55
- Zarnitsyn VG, Prausnitz MR. Physical parameters influencing optimization of ultrasound-mediated DNA transfection. *Ultrasound Med Biol* 2004;**30**:527–38
- Pardridge WM. The blood-brain barrier: bottleneck in brain drug development. *NeuroRx* 2005;**2**:3–14
- Timbie KF, Mead BP, Price RJ. Drug and gene delivery across the blood-brain barrier with focused ultrasound. *J Control Release* 2015;**219**:61–75
- Pfaffenberger S, Devic-Kuhar B, Kastl SP, Huber K, Maurer G, Wojta J, Gottsauner-Wolf M. Ultrasound thrombolysis. *Thromb Haemost* 2005;**94**:26–36
- Petit B, Bohren Y, Gaud E, Bussat P, Arditi M, Yan F, Tranquart F, Allémann E. Sonothrombolysis: the contribution of stable and inertial cavitation to clot lysis. *Ultrasound Med Biol* 2015;**41**:1402–10
- Nederhoed JH, Ebben HP, Slikkerveer J, Hoksbergen AWJ, Kamp O, Tangelder GJ, Wisselink W, Musters RJP, Yeung KK. Intravenous targeted microbubbles carrying urokinase versus urokinase alone in acute peripheral arterial thrombosis in a porcine model. *Ann Vasc Surg* 2017;**44**:400–7
- Cui H, Zhang T, Yang X. Laser-enhanced cavitation during high intensity focused ultrasound: an *in vivo* study. *Appl Phys Lett* 2013;**102**:133702
- Jo J, Yang X. Laser-enhanced high-intensity focused ultrasound heating in an *in vivo* small animal model. *Appl Phys Lett* 2016;**109**:213702
- Cui H, Yang X. Enhanced-heating effect during photoacoustic imaging-guided high-intensity focused ultrasound. *Appl Phys Lett* 2011;**99**:231113
- Hoffman HJ, Telfair WB. Photospallation: a new theory and mechanism for mid-infrared corneal ablations. *J Refract Surg* 2000;**161**:90–4
- Vogel A, Venugopalan V. Mechanisms of pulsed laser ablation of biological tissues. *Chem Rev* 2003;**103**:577–644
- Paltauf G, Schmidt-Kloiber H. Photoacoustic cavitation in spherical and cylindrical absorbers. *Appl Phys A* 1999;**68**:525–31
- Li S, Qin Y, Wang X, Yang X. Bubble growth in cylindrically-shaped optical absorbers during photo-mediated ultrasound therapy. *Phys Med Biol* 2018;**63**:125017
- Qin Y, Yu Y, Xie X, Zhang W, Fu J, Paulus YM, Yang X, Wang X. The effect of laser and ultrasound synchronization in photo-mediated ultrasound therapy. *IEEE Trans Biomed Eng* 2020;**67**:3363–70
- Qin Y, Yu Y, Fu J, Wang M, Yang X, Wang X, Paulus YM. Photo-mediated ultrasound therapy for the treatment of retinal neovascularization in rabbit eyes. *Lasers Surg Med* 2022;**54**:747–57
- Zhang H, Xie X, Li J, Qin Y, Zhang W, Cheng Q, Yuan S, Liu Q, Paulus YM, Wang X, Yang X. Removal of choroidal vasculature using concurrently applied ultrasound bursts and nanosecond laser pulses. *Sci Rep* 2018;**8**:12848

21. Wang M, Qin Y, Wang T, Orringer JS, Paulus YM, Yang X, Wang X. Removing subcutaneous microvessels using photo-mediated ultrasound therapy. *Lasers Surg Med* 2020;**52**:984–92
22. Singh R, Jo J, Riegel M, Forrest ML, Yang X. The feasibility of ultrasound-assisted endovascular laser thrombolysis in an acute rabbit thrombosis model. *Med Phys* 2021;**48**:4128–38
23. Singh R, Yang X. A novel ultrasound-assisted laser technique to remove atherosclerotic plaques. *J Acoust Soc Am* 2022;**151**:A109
24. Hu Z, Zhang H, Mordovanakis A, Paulus YM, Liu Q, Wang X, Yang X. High-precision, non-invasive anti-microvascular approach via concurrent ultrasound and laser irradiation. *Sci Rep* 2017;**7**:40243
25. Gao F, Hu Y, Hu H. Asymmetrical oscillation of a bubble confined inside a micro pseudoelastic blood vessel and the corresponding vessel wall stresses. *Int J Solids Struct* 2007;**44**:7197–212
26. Hosseinkhah N, Hynynen K. A three-dimensional model of an ultrasound contrast agent gas bubble and its mechanical effects on microvessels. *Phys Med Biol* 2012;**57**:785–808
27. Hosseinkhah N, Chen H, Matula TJ, Burns PN, Hynynen K. Mechanisms of microbubble–vessel interactions and induced stresses: a numerical study. *J Acoust Soc Am* 2013;**134**:1875–85
28. Singh R, Wang X, Yang X. Cavitation induced shear and circumferential stresses on blood vessel walls during photo-mediated ultrasound therapy. *AIP Adv* 2020;**10**:125227
29. Keller JB, Miksis M. Bubble oscillations of large amplitude. *J Acoust Soc Am* 1980;**68**:628–33
30. Church CC. Prediction of rectified diffusion during nonlinear bubble pulsations at biomedical frequencies. *J Acoust Soc Am* 1988;**83**:2210–7
31. Fyrrillas MM, Szeri AJ. Dissolution or growth of soluble spherical oscillating bubbles: the effect of surfactants. *J Fluid Mech* 1995;**289**:295–314
32. VanBavel E. Effects of shear stress on endothelial cells: possible relevance for ultrasound applications. *Prog Biophys Mol Biol* 2007;**93**:374–83
33. Zhong P, Zhou Y, Zhu S. Dynamics of bubble oscillation in constrained media and mechanisms of vessel rupture in SWL. *Ultrasound Med Biol* 2001;**27**:119–34
34. Karthikesh MS, Wu S, Singh R, Paulus Y, Wang X, Yang X. Effect of photo-mediated ultrasound therapy on nitric oxide and prostacyclin from endothelial cells. *Appl Sci* 2022;**12**:2617
35. Hazlewood D, Yang X. Enhanced cavitation activity in a slab-shaped optical absorber during photo-mediated ultrasound therapy. *Phys Med Biol* 2020;**65**:055006
36. Wang L, Jacques SL, Zheng L. MCML – Monte Carlo modeling of light transport in multi-layered tissues. *Comput Methods Programs Biomed* 1995;**47**:131–46
37. Qin Y, Yu Y, Fu J, Xie X, Wang T, Woodward MA, Paulus YM, Yang X, Wang X. Photo-mediated ultrasound therapy for the treatment of corneal neovascularization in rabbit eyes. *Transl Vis Sci Technol* 2020;**9**:16
38. Zhang W, Qin Y, Xie X, Hu Z, Paulus YM, Yang X, Wang X. Real-time photoacoustic sensing for photo-mediated ultrasound therapy. *Opt Lett* 2019;**44**:4063–6
39. Cui H, Yang X. Laser enhanced high-intensity focused ultrasound thrombolysis: an in vitro study. *J Acoust Soc Am* 2013;**133**:E1123–8
40. Jo J, Forrest ML, Yang X. Ultrasound-assisted laser thrombolysis with endovascular laser and high-intensity focused ultrasound. *Med Phys* 2021;**48**:579–86
41. Kearon C, Akl EA, Ornelas J, Blaivas A, Jimenez D, Bounameaux H, Huisman M, King CS, Morris TA, Sood N, Stevens SM, Vintch JRE, Wells P, Woller SC, Moores L. Antithrombotic therapy for VTE disease: CHEST guideline and expert panel report. *Chest* 2016;**149**:315–52
42. Daley MJ, Murthy MS, Peterson EJ. Bleeding risk with systemic thrombolytic therapy for pulmonary embolism: scope of the problem. *Ther Adv Drug Safety* 2015;**6**:57–66
43. Parikh S, Motarjeme A, McNamara T, Raabe R, Hagspiel K, Benenati JF, Sterling K, Comerota A. Ultrasound-accelerated thrombolysis for the treatment of deep vein thrombosis: initial clinical experience. *J Vasc Interv Radiol* 2008;**19**:521–8
44. Den Heijer P, Van Dijk RB, Pentinga ML, Hillege HL, Lie KI. Laser thrombolysis in acute myocardial infarction: results of a clinical feasibility study. *J Interv Cardiol* 1994;**7**:525–34
45. Maxwell AD, Owens G, Gurm HS, Ives K, Myers DD Jr, Xu Z. Noninvasive treatment of deep venous thrombosis using pulsed ultrasound cavitation therapy (histotripsy) in a porcine model. *J Vasc Interv Radiol* 2011;**22**:369–77
46. Shangguan HQ, Gregory KW, Casperson LW, Prah SA. Enhanced laser thrombolysis with photomechanical drug delivery: an in vitro study. *Lasers Surg Med* 1998;**23**:151–60
47. Hoole SP, Bambrough P. Recent advances in percutaneous coronary intervention. *Heart* 2020;**106**:1380–6
48. Cook SL, Eigler NL, Shefer A, Goldenberg T, Forrester JS, Litvack F. Percutaneous excimer laser coronary angioplasty of lesions not ideal for balloon angioplasty. *Circulation* 1991;**84**:632–43
49. Sintek M, Coverstone E, Bach R, Zajarias A, Lasala J, Kurz H, Kennedy K, Singh J. Excimer laser coronary angioplasty in coronary lesions: use and safety from the NCDR/CATH PCI Registry. *Circ Cardiovasc Interv* 2021;**14**:e010061
50. Farny CH, Wu T, Holt RG, Murray TW, Roy RA. Nucleating cavitation from laser-illuminated nano-particles. *Acoust Res Lett Online* 2005;**6**:138–43
51. Wu T, Farny CH, Roy RA, Holt RG. Modeling cavitation nucleation from laser-illuminated nanoparticles subjected to acoustic stress. *J Acoust Soc Am* 2011;**130**:3252–63
52. Wei CW, Xia J, Lombardo M, Perez C, Arnal B, Larson-Smith K, Pelivanov I, Matula T, Pozzo L, O'Donnell M. Laser-induced cavitation in nanoemulsion with gold nanospheres for blood clot disruption: in vitro results. *Opt Lett* 2014;**39**:2599–602
53. Li Y, Song Y, Li R, Jia W, Zhang F, Hu X, Chou L, Zhou Q, Chen Z. High speed photo-mediated ultrasound therapy integrated with OCTA. *Sci Rep* 2022;**12**:19916
54. Avery RL, Pearlman J, Pieramici DJ, Rabena MD, Castellarin AA, Nasir MA, Giust MJ, Wendel R, Patel A. Intravitreal bevacizumab (Avastin) in the treatment of proliferative diabetic retinopathy. *Ophthalmology* 2006;**113**:1695.e1–15
55. Maguire MG, Martin DF, Ying GS, Jaffe GJ, Daniel E, Grunwald JE, Toth CA, Ferris FL III, Fine SL. Five-year outcomes with anti-vascular endothelial growth factor treatment of neovascular age-related macular degeneration: the comparison of age-related macular degeneration treatments trials. *Ophthalmology* 2016;**123**:1751–61
56. Yang N, Fan CM, Ho CK. Review of first year result of photodynamic therapy on age-related macular degeneration in chinese population. *Eye* 2006;**20**:523–6
57. Petersen B, Wiegell SR, Wulf HC. Light protection of the skin after photodynamic therapy reduces inflammation: an unblinded randomized controlled study. *Br J Dermatol* 2014;**171**:175–8
58. Sramek C, Paulus Y, Nomoto H, Huie P, Brown J, Palanker D. Dynamics of retinal photocoagulation and rupture. *J Biomed Opt* 2009;**14**:034007
59. Guyer DR, D'Amico DJ, Smith CW. Subretinal fibrosis after laser photocoagulation for diabetic macular edema. *Am J Ophthalmol* 1992;**113**:652–6
60. Lewen RM. Subretinal neovascularization complicating laser photocoagulation of diabetic maculopathy. *Ophthalmic Surg* 1988;**19**:734–7
61. Morelli JG, Tan OT, Garden J, Margolis R, Seki Y, Boll J, Carney JM, Anderson RR, Furumoto H, Parrish JA. Tunable dye laser (577 nm) treatment of port wine stains. *Lasers Surg Med* 1986;**6**:94–9
62. Savas JA, Ledon JA, Franca K, Chacon A, Nouri K. Pulsed dye laser-resistant port-wine stains: mechanisms of resistance and implications for treatment. *Br J Dermatol* 2013;**168**:941–53
63. Zhong SX, Liu YY, Yao L, Song Y, Zhou JF, Zu JJ, Li SS. Clinical analysis of port-wine stain in 130 Chinese patients treated by long-pulsed 1064-nm Nd: YAG laser. *J Cosmet Laser Ther* 2014;**16**:279–83
64. Van Drooge AM, Bosveld B, Van Der Veen JP, De Rie MA, Wolkerstorfer A. Long-pulsed 1064 nm Nd:YAG laser improves hypertrophic port-wine stains. *J Eur Acad Dermatol Venereol* 2013;**27**:1381–6
65. Neiman HL, Vogelzang RL. Diagnostic ultrasound: a review of the state of the art. *Arch Dermatol* 1984;**120**:248–53
66. Şen T, Tüfekçioğlu O, Koza Y. Mechanical index. *Anatol J Cardiol* 2015;**15**:334–6